Nitrogen footprint in a long-term observation of forest growth over the twentieth century

Jean-Daniel Bontemps, Jean-Christophe Hervé, Jean-Michel Leban, Jean-François Dhôte

NITROGEN FOOTPRINT IN A LONG-TERM OBSERVATION OF FOREST GROWTH OVER THE TWENTIETH CENTURY

Jean-Daniel BONTEMPS[1,*], Jean-Christophe HERVE[2], Jean-Michel LEBAN[3], Jean-François DHÔTE[4]

[1]AgroParisTech, ENGREF, UMR 1092 INRA/AgroParisTech Laboratoire d'Etude des Ressources Forêt-Bois (LERFoB), 14 rue Girardet, 54000 Nancy, France.

[2]Inventaire Forestier National (IFN), Direction Technique, Château des Barres, 45290 Nogent-sur-Vernisson, France.

[3]INRA, Centre de Nancy, UMR 1092 INRA/AgroParisTech Laboratoire d'Etude des Ressources Forêt-Bois (LERFoB), 54280 Champenoux, France.

[4]Office National des Forêts (ONF), Direction Technique et Commerciale Bois, Boulevard de Constance, 77300 Fontainebleau, France. jean-francois.dhote@onf.fr

***Corresponding author:** Jean-Daniel BONTEMPS, jean-daniel.bontemps@engref.agroparistech.fr

ABSTRACT

Environmental drivers of forest productivity increases have been much debated. Evidence for the suggested role of increasing nitrogen supply is lacking over long-term time scales. Tracking the footprint of environmental factors by using long-term growth records may thus prove decisive.

We analysed growth chronologies of common beech in 2 areas of contrasting nutritional status in France. Dominant height growth was used as a proxy for productivity. Growth was compared between old and young paired stands sampled at the same sites to factor out effects of ageing and site. Growth chronologies were estimated with a statistical modelling procedure. The environmental causality of growth changes was addressed by combining (i) a comparison of growth changes between regions, (ii) a regional comparison of growth chronologies with chronologies of environmental factors, and (iii) growth-environment relationships established from climate/soil data.

Historical growth increases followed very similar courses in the 2 areas. Remarkably, the magnitude of change was 50% lower in the area that had reduced nutritional status and nitrogen deposition. Historical variations in environmental factors and growth were congruent with the roles of nitrogen availability and deposition, and of atmospheric CO_2 increase. Low-frequency variations in climate and growth were not coincident. However, our analysis demonstrated the role of climatic anomalies in short-term growth variations. Growth-environment relationships further indicated a nitrogen constraint.

These observations corroborate the enhancing role of increased nitrogen availability on forest biomass accumulation previously reported in ecosystem experiments and process-based modelling explorations.

Keywords: forest growth, long-term trends, nitrogen, climate, carbon dioxide, *Fagus sylvatica*.

INTRODUCTION

Increases in temperate and boreal forest productivity have been evidenced over the past several decades (Boisvenue and Running 2006; Spiecker et al. 1996). Because there are several potential environmental drivers, including increased atmospheric CO_2 concentration, climate change, and nitrogen deposition, the role of each has been much debated (Hyvönen et al. 2007). Contributing to the complexity of the issue are potentially positive and negative interactions among these factors, dependencies of responses on environmental limitations of the ecosystems under consideration, and delays in ecosystem response (Ollinger et al. 2002).

Existing contributions on environmental factor effects on increased productivity are consistently indecisive. Retrospective growth studies have demonstrated a global fingerprint of climate change (Boisvenue and Running 2006; Esper et al. 2002). The enhancing effect of CO_2 increase on productivity has been putatively inferred by observations (e.g. Lamarche et al. 1984) and ecosystem experiments (Norby et al. 2005), but this effect has also been questioned (Jacoby and d'Arrigo 1997; Körner et al. 2005). There is growing awareness of the fact that impacts of CO_2 increase may depend on ecosystem nitrogen availability (Nowak et al. 2004). Reports indicate that increasing nitrogen supply throughout Europe has stimulated past growth (Kahle et al. 2008a) and also has effects on recent growth rates (e.g. Solberg et al. 2009). However, positive effects of nitrogen deposition have been challenged (Nadelhoffer et al. 1999). Negative impacts of nitrogen deposition are also supported by evidences of nitrate leaching and soil acidification (Aber et al. 2003; Macdonald et al. 2002), which stem from excess nitrogen, called nitrogen saturation (Aber et al. 1998). The role of nitrogen availability thus remains controversial.

There have been 3 approaches to determining the contribution of environmental factors to productivity changes: ecosystem experiments, process-based modelling analyses, and observations of past growth. Ecosystem experiments have included nitrogen fertilization/suppression manipulations (Wright and Rasmussen 1998) and free air CO_2 enrichment (FACE, Hendrey et al. 1999). Interactions between these factors have also been explored experimentally (Nowak et al. 2004). These experiments have limitations as they may reveal (or miss) transient (or delayed) responses due to their short duration. They also diverge from real conditions when factors are manipulated (e.g., Högberg et al. 2006). Process-based models encompass fundamental ecosystem processes that have explicit dependence on the environment (Constable and Friend 2000; Landsberg 2003; Luckai and Laroque 2002). They have thus contributed to quantifying ecosystem responses to environmental changes (van Oijen et al. 2008) and to the identification of key control processes

(e.g. Medlyn et al. 2000). However, their predictive ability is challenged by the frequently incomplete description of processes and uncertainties in parameter estimates (Luckai and Laroque 2002; Landsberg 2003; Mäkelä et al. 2000). Growth records offer a unique procedure for tracking past long-term dynamics of ecosystem productivity as an integrated response to environmental changes. They are thus crucial for testing the outcomes of short-term experiments and model explorations. In the growth record approach, environmental causality is investigated by comparing temporal and spatial patterns of environmental factors and productivity (Jacoby and d'Arrigo 1997). Empirical productivity-environment relationships can also aid in the determination of limiting factors (Seynave et al. 2008).

However, the success of this observation-as-a-baseline strategy has not been comprehensively successful to date. Dendrochronology has contributed mainly to documenting growth trends from tree core samplings (Boisvenue and Running 2006; Jacoby and d'Arrigo 1997). Yet, radial growth indicators are sensitive to between-tree competition and may reflect past disturbances or silvicultural shifts. Whether they accurately depict ecosystem productivity is also an issue for debate (Bouriaud et al. 2005). Productivity-oriented indicators have also been investigated in Europe (Spiecker et al. 1996), but growth chronologies have seldom been determined, and the heterogeneity of approaches has hindered regional comparisons. Hence, it has not been possible to attribute causality to temporal shifts in environmental factors. To our knowledge, only 2 observational studies have addressed growth trends and their causality so far. Nellemann and Thomsen (2001) compared radial growth chronologies of Norway spruce over a gradient of nitrogen deposition in Norway. However, stand density was not controlled, and other drivers were not addressed. Kahle et al. (2008b) compared tree height growth data with climate and foliar nitrogen trends in 3 northern European species. Confounding of factors, however, prevented unambiguous interpretation and attribution of causality. In addition, both analyses were restricted to medium-term growth variations.

We previously developed a method for quantifying long-term growth trends in even-aged stands (Bontemps et al. 2009) using: (i) dominant height growth reconstructed from stem analyses to serve as a proxy for aboveground productivity (Assmann 1970), (ii) the paired-plots sampling method, which allows for comparisons between young and old stands located in the same site conditions, and (iii) a statistical modelling approach for estimating growth chronology, factoring out the effects of ontogeny and site. We demonstrated a productivity increase of 50% throughout the twentieth century for common beech (*Fagus sylvatica* L.) in north-eastern France, mostly occurring in the 1950-1980s. The pattern we observed suggested a potential role for nitrogen deposition, in the frame of the nitrogen limitation hypothesis (Johnson 2006).

Accordingly, we repeated the study in an area with sites of contrasting nutritional status and

nitrogen deposition level. Our objectives were: (i) to determine the regional variation in past productivity changes, (ii) to draw inferences on the environmental drivers of these changes, based on their documented historical variations and regional growth-environment relationships, and (iii) to test the relevance of the nitrogen driver hypothesis.

MATERIALS

Study area and forest species

The present study was based on temporary plots. We focused on even-aged stands of common beech in the northern plains sector of the species distribution (Seynave et al. 2008). To ensure management continuity through time, we restricted the sampling to State Forests. Beech has not been subjected to genetic selection programmes, and natural regeneration predominates, indicating that any historical changes are highly unlikely to be the result of human technical intervention. In addition, past disturbances caused by silvicultural practice were unlikely to have impacted the present sample, as beech stands are attested to have been managed as high forests from establishment onwards (Hüffel 1926). The historical intensity of forest management is moreover considered moderate for this species (Polge 1981).

We selected the north-western Atlantic area (sample 2) of common beech distribution in France to complement the initial north-eastern sampling area (sample 1), because soils of the Atlantic area have lower nutritional status (European Commission 2005) and because current rates of total atmospheric nitrogen deposition (4-7 $kg.ha^{-1}.year^{-1}$) in western France are lower than in eastern areas (8-13 $kg.ha^{-1}.year^{-1}$) (Croisé et al. 2005).

Dominant height as a productivity indicator

Dominant height corresponds to the height of the most vigorous trees in a pure and even-aged stand, and was defined as the mean height of the 100 thickest trees in 1 ha. Dominant height and aboveground net primary productivity (wood ANPP) are closely related, regardless of site fertility and stand density conditions (Assmann 1970). The reason for this lies in the insensitivity of both dominant height (Lanner 1985) and ANPP (law of constant yield, Bormann and Gordon 1984) to density within the usual range of closed-canopy stands. Hence, dominant height growth rate was used as a proxy for forest productivity. Stem analysis allows individual tree height growth to be reconstructed (Curtis 1964). We applied the procedure to samples of dominant trees. For each tree,

the first 2 or 3 disc sections were sawn every 4 m along logs beginning 0.30 m above ground level, and then every 2 m in the upper part of the stem to the terminal bud.

Sampling design: controlling for tree age and site conditions

We partitioned out effects on growth of historical changes, ontogeny and site fertility by using a paired-plots sampling design, in which plots were sampled in pairs of young and old stands located within the same sites. This sampling also ensures some homogeneity of historical management and genetic similarity among trees. To encompass site variation within each area, we sampled around 15 stand pairs/area. Candidate pairs were first identified using forest management and geological maps. Old stands were selected around the standard rotation age (150–180 years) and young stands were half this age (70–80 years). Pairs were sampled after controlling for stand structure, species homogeneity, permanent environmental characteristics (topography, parent rock and soil) and current nutritional status (humus forms and summer surveys of understory vegetation).

Growth data

Information on the 14 pairs in sample 1 is provided in Bontemps et al. (2009). Sample 2 comprised 15 pairs whose location and age are indicated in the Online Resource. Both samples are mapped in **Figure 1**. In each stand, dominant trees (defined above) were sampled following the protocol of Duplat and Tran-Ha (1997); first, the five thickest trees in a circular plot of 0.06 ha were selected to avoid local sampling bias (Pierrat et al. 1995). Next, the first, third and fifth thickest trees were selected for stem analysis to reduce the sampling effort. Individual growth curves of these trees were averaged to give a plot mean curve. In total, 174 stem analyses were performed. From samples 1 and 2, respectively, we obtained 356 and 390 growth increments, covering on average 7.2 and 8.3 years (SD: 3.9 and 4.7 years), respectively. Height curves plotted for each sample are compared between generations in **Figure 2**.

Environmental data

In all plots, current local nutrition and water status were documented from soil analyses and understory vegetation-based indicators. Indicators of mean climate (1961–1990) at 1 km spatial resolution were extracted for each stand pair (mean coordinates of the 2 plots) from the AURELHY model (Bénichou and Le Breton 1987).

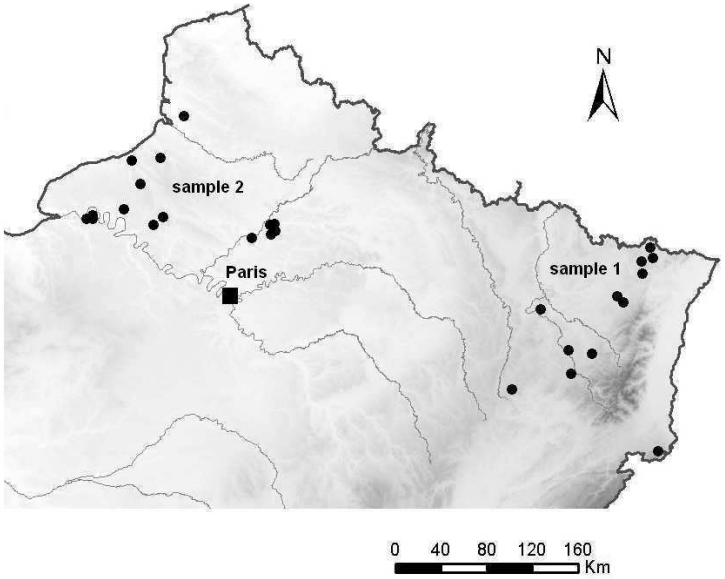

Fig. 1 Location of samples 1 and 2. Each dot indicates a stand-pair located in either north-eastern or north-western France.

a **b**

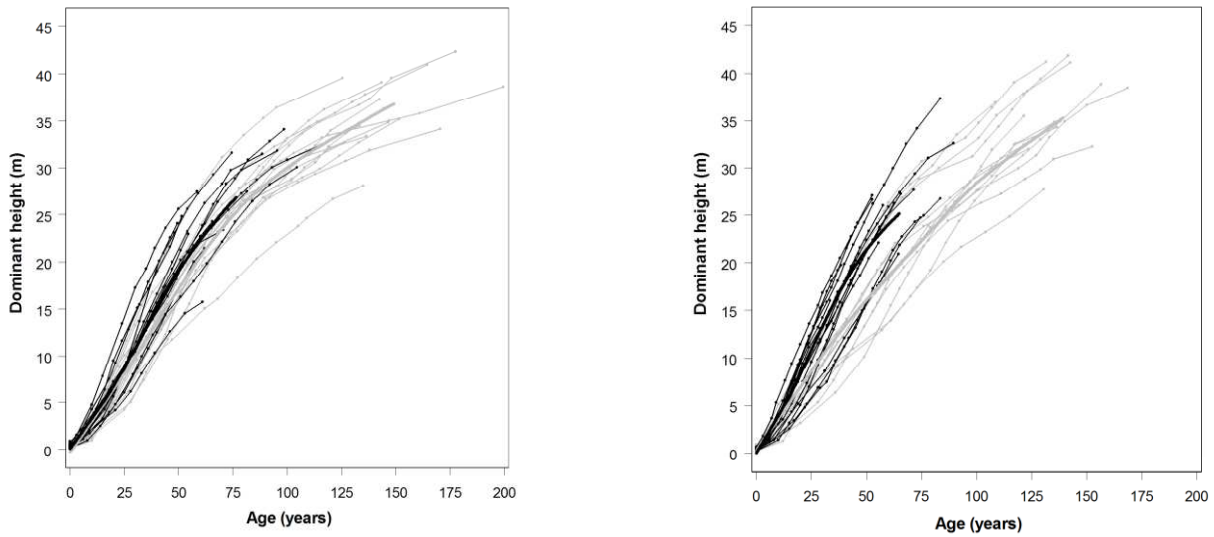

Fig. 2 Dominant height growth curves. a: sample 1, b: sample 2, grey lines: growth curves of the older generation, black lines: growth curves of the younger generation. Growth curves are smoothed by generation for each sample (LOESS locally weighted regression smoothing) through the mean generation age. Grey thick line: older generation fitted curve, black thick line: younger generation fitted curve.

Soil analyses and vegetation-based indicators

Soil layer textures were analysed to estimate the 1 m depth soil water capacity (SWC100). Cation (cobaltihexamin extraction at soil pH), pH, total nitrogen (N), organic carbon (C) and phosphorus (Phos, sodium bicarbonate extraction at pH 8.5 or Olsen's method) concentrations were also measured in each soil layer to a depth of 30 cm. C:N ratio, base cation concentration (S=Ca+K+Mg+Na), cation exchange capacity (CEC=S+Al+H+Fe+Mn) and base saturation rate (S:CEC) were also computed. Selected vegetation-based Ellenberg indicators (Ellenberg et al. 1992) included nitrogen (Nel), basicity (Rel), humidity (Fel) and ambient light (Lel) values. According to this system, each plant species is rated on an increasing relative 9-point scale for each factor. Averages for each indicator were computed over each vegetation survey. Soil C:N ratio and the nitrogen Ellenberg indicator have been correlated with soil nitrogen mineralization (Janssen 1996; Schaffers and Sýkora 2000) and nitrification (Andrianarisoa et al. 2009; Schaffers and Sýkora 2000) and were consequently selected as measures of soil nitrogen availability.

Mean climate data

Mean climate indicators included monthly precipitation (P), minimum, maximum and mean monthly temperatures (Tn, Tx, Tm) and annual number of freezing days (NFD). Monthly potential evapotranspiration (PET) values were calculated from temperature and solar radiation (Rad; Piedallu and Gégout 2007). Monthly water balances (WB) were calculated as P-PET. Monthly soil water budgets (SWB) and soil water deficits (SWD) were calculated from SWC100, P and PET. Monthly indicators were indexed by corresponding calendar month numbers (e.g. Tx7 for maximum temperatures in July).

Regional chronologies of environmental factors

We assembled data for past climate, atmospheric CO_2 concentration and nitrogen deposition. As is general in retrospective sampling studies performed in temporary plots, no environmental monitoring has been conducted in the past, and information on the historical nutritional status of these forest stands is absent. The 1901–2000 chronologies for precipitation and mean temperature were extracted for each stand pair from the CRU TS 1.2 monthly dataset for Europe at a 10′ angular (approximately 15 km) spatial resolution (Mitchell et al. 2004) and averaged over each regional sample. Geographic variation of CO_2 concentration is reportedly marginal (Chahine et al. 2005; airs.jpl.nasa.gov/AIRS_CO2_Data/). A single chronology was thus computed from CDIAC datasets (cdiac.ornl.gov/). Although spatial patterns of recent deposition are known from monitoring networks (Holland et al. 2005), European long-term records of nitrogen deposition remain

anecdotal (e.g. Blake et al. 1999). Recent NO_3^-/NH_4^+ bulk deposition in the open field and throughfall deposition have been monitored on a monthly basis in France on the CATANEAT forest network, a subset of the RENECOFOR network (French level-II plots of the ICP forests network; Croisé et al. 2005; Ulrich 1999). Bulk deposition is defined as the total deposition of material (wet-only deposition, dry particles, gases and fine aerosols) to a continuously-open sampler, and it is generally lower than the total deposition intercepted by vegetated surfaces (Dämmgen et al. 2005). Because it is independent from forest canopy structure and composition, it can be modelled and spatially extrapolated using abiotic predictors. Bulk depositions of NO_3^- and NH_4^+ monitored in the CATANEAT network over the period 1993–1998 have been modelled as a function of elevation, monthly precipitation and period of the year. These models have been validated against deposition data for the period 1999–2001 and they have shown a good predictive ability (Croisé et al. 2005). We applied these models to the 1993–1998 CRU climate data extracted for each stand pair sampled, and plot elevations. Predictions from these models were averaged over each regional sample. EMEP data for nitrogen deposition were not used, as they apply at a coarse spatial scale (50km x 50 km grid) and have been found to partially capture the spatial distribution of deposition in France (Croisé et al. 2005).

Posterior control of stand pairing and variations in site conditions

The accuracies of pairings were assessed by tracking inappropriately-matched individual pairings and systematic between-generation differences in soil-related indicators. Systematic differences were tracked using two-sided paired *t* tests. Accuracies of pairings were confirmed in sample 1 (Bontemps et al. 2009) and in sample 2 for both criteria.

A selection of important environmental indicators is presented in **Table 1**. In agreement with European soil maps (European Commission 2005), soil indicators demonstrated a lower nutritional status in sample 2. Phosphorus concentrations were very similar between samples. Larger annual temperature amplitude with colder winter and early growing season occurred in sample 1 (semi-continental). However, mean temperatures of growing seasons were equivalent. Soil water capacities were similar in both samples. Precipitation was 140 mm higher in sample 1; the difference was distributed mostly over the growing season (+110 mm in April-September, +60 mm during summer). This resulted in an end-summer SWB 50% lower in sample 2 than in sample 1.

Environmental indicator		Sample 1	Sample 2
Nutritional resources			
pH *		5.0 (0.9)	4.3 (0.8)
Rel (Ellenberg scale)	Basicity level	5.1 (1.1)	4.5 (1.2)
S:CEC *	Base saturation rate	0.47 (0.34)	0.34 (0.23)
C:N *	Carbon to nitrogen ratio	16.2 (2.8)	17.5 (2.9)
Nel (Ellenberg scale)	Nitrogen level	5.1 (0.8)	4.9 (0.8)
Phos (g .kg^{-1}) *	Phosphorus concentration	0.041 (0.037)	0.036 (0.027)
Energy resources			
Rad (MJ .m^{-2})	Annual radiations	4080 (305)	3940 (70)
Tn (°C)	Annual minimum temperature	4.6 (0.4)	5.9 (0.3)
Tx (°C)	Annual maximum temperature	13.5 (0.5)	14.0 (0.7)
NFD (days)	Number of freezing days	90.7 (10.2)	54.0 (5.6)
Tm4-9 (°C)	Mean temperature/April-September	14.2 (0.15)	14.2 (0.6)
Tn4-5 (°C)	Mean temperature/April-May	5.1 (0.4)	5.8 (0.3)
Tx6-8 (°C)	Maximum temperature/June-August	22.7 (0.7)	21.5 (1.1)
Water resources			
SWC100 (mm)	Soil water capacity at 1m depth	136 (37)	126 (41)
P (mm)	Annual precipitation	928 (61)	786 (95)
P-PET (mm)	Annual water balance	300 (58)	144 (111)
P4-9 (mm)	Precipitation/April-September	463 (37)	355 (30)
P6-8 (mm)	Precipitation/June-August	236 (19)	172 (14)
(P-PET) 6-8 (mm)	Water balance/June-August	-100 (24)	-149 (21)
SWB8 (mm)	Soil water budget/end August	74 (48)	33 (17)
Fel (Ellenberg scale)	Humidity level	5.3 (0.2)	5.4 (0.4)

Table 1. Environmental indicators for growth samples. Main indicator averages were computed for each sample. Figures given in parentheses indicate standard deviations of indicators. Mean climate indicators refer to the period 1961–1990. * values of indicators for the first soil layer.

MODELLING APPROACH

Historical changes in dominant height growth rate

Removing effects of ageing and site fertility on growth was a requirement for estimating changes in growth rate over time. Dominant height growth was analysed as a multiplicative function of the effects of developmental stage (H_0, function f_1), site conditions (dummy coefficient S_b) at a base date (t_b) and running calendar year (f_2). The model was expressed in continuous time:

$$\frac{dH_0}{dt} = f_1(H_0)\, S_b\ f_2(t - t_b) \qquad (1)$$

The function f_2 is such that $f_2(t_b) = 1$, with t_b taken as 1900. Equation (1) was integrated with respect to time, to be fitted to the pluri-annual increment data:

$$H_0(t) = F_1^{-1}\left[F_1(H_0(t_{-1})) + S_b\ (F_2(t) - F_2(t_{-1}))\right] \qquad (2)$$

where $F_1 = \int \frac{du}{f_1(u)}$ and $F_2 = \int f_2(v)\, dv$ (u and v are dummy variables of integration)

The pattern of growth remained sigmoid in old and young stand generations (**Figure 2**). Therefore, sigmoid equations were used to model the effect of developmental stage. As an upper limit to height growth was undetected in these data, we selected three 3-parameter asymptotic growth equations showing slow convergence: the Richards, the Korf, and the Hossfeld equations (Zeide 1993). Their basic expression is given by:

$$\frac{dH_0}{dt} = R\ f(H_0, K, m) \qquad (3)$$

They were parameterized so that R ($m.yr^{-1}$) is the maximal growth rate, K (m) is the asymptotic height and m is a shape parameter (dimensionless). Parameter S_b was assimilated to R, and f_1 to f. The asymptotic height parameter K in the growth equation may also depend on site conditions. Hence, its pair-wise variation was tested. As the uppermost sections of the height curves are lacking for the young stand generation (**Figure 2**), it was however impossible to accurately test whether this

parameter also changed over time. The effect of date (f_2) was represented by a polynomial cubic spline function for assessing growth fluctuations on a decennial scale. Cubic splines were chosen to prevent excessive oscillations of ordinary polynomials. Mathematical expressions for the selected growth equations (f_1 and F_1^{-1}) and the effects of calendar date (f_2) are given in the Online Resource. An in-depth justification of the model structure is provided in Bontemps et al. (2009).

Data are longitudinal and have 2 hierarchical levels (pairs as level 1, stands within pairs as level 2) at which model parameters can vary. The model was fitted using a non-linear hierarchical mixed-effects model approach (Lindström and Bates 1990). Level 1 and 2 variations in maximal growth rate S_b should correspond to the effect of site and residual within-pair site differences, and were tested. Level 1 variation of K and its correlation with S_b were also tested. The random parameters were assumed to follow Gaussian distributions (Lindström and Bates 1990):

$$S_b \sim N\left(S_{b0}, \sigma_{Sb,1} + \sigma_{Sb,2}\right), K_1 \sim N\left(K_0, \sigma_{K,1}\right), \rho_1 = \mathrm{cor}\left(S_b, K\right) \qquad (4)$$

where, $\sigma_{Sb,1}$ and $\sigma_{Sb,2}$ are random standard-deviations of S_b at levels 1 and 2, $\sigma_{K,1}$ that of K at level 1, ρ_1 is their correlation and S_{b0} and K_0 are fixed components of S_b and K.

Equation (2) was fitted to increments (forward difference data) using the maximum likelihood criterion of the *nlme* procedure in S-PLUS software (Pinheiro and Bates 2000). Errors were assumed Gaussian and their standard-deviation (residual standard error) was assumed to be proportional to a power (λ) function of the expected height increment. Selection of a growth equation and adequate parameterization for random effects and cubic splines were performed using the AIC criterion and the Khi-2 likelihood ratio test (LRT) for nested models.

Growth-environment relationships

To identify environmental factor constraints on growth, relationships between maximal height growth rate (S_b) and soil and mean climate indicators relative to each plot were investigated in each regional sample (28 or 30 estimates of parameter S_b and environmental indicators, depending on the sample) and over the combined dataset. To make the analysis comparable between the 2 regions, estimates of S_b were obtained using a common growth equation (see Results). Growth-environment relationships were established in 2 steps. First, correlations between maximal growth rate and environmental indicators were systematically computed and tested using Pearson's correlation *t* tests at a minimum significance level of 0.05. Significant correlations of the same sign over successive months were interpreted as seasonal patterns. To reduce inflation in variable numbers,

sums (precipitations) or means (temperatures) of monthly climatic indicators were calculated over the corresponding periods whenever seasonal patterns were observed. Correlations between these seasonal indicators and maximal growth rates were again computed. Secondly, we built a multiple linear regression model of maximal growth rate, starting with indicators with most significant correlations. Indicators with weaker correlations were incorporated into the regression model until a minimum level of significance of 0.05 was exceeded. When both monthly and seasonal indicators of the same climatic variable were significant in the regressions, we systematically retained the model including seasonal indicators (**Table 4**), considered to be biologically more meaningful.

RESULTS

Historical changes in dominant height growth rate

Pair-wise comparisons of dominant height at the final ages of the younger stands indicated that younger stands were systematically taller than the older ones (**Figure 2**). Mean differences were highly significant, and were up to 5.7 m in sample 1 ($p < 10^{-4}$, mean comparison age 75.4 years) and 2.2 m in sample 2 ($p < 10^{-3}$, mean comparison age 73.5 years). The difference was significantly smaller in sample 2 than in sample 1 ($p = 0.002$).

Main characteristics of the growth models are reported in **Table 2**. The Hossfeld and Korf equations proved to be the most accurate for samples 1 and 2, respectively. In sample 2, the Hossfeld equation provided a lower but nevertheless very close fitting accuracy (+4.5 points in AIC, comparable RSE, **Table 2**). The random structure selected was the same for both samples: a level 1 random variation of parameters S_b and K (the correlation between S_b and K was not significant), and a level 2 variation of S_b (**Table 2**). Level 1 standard-deviations of random effects were below 10% for K and ca. 15% for S_b. Cubic splines for the effect of date were best parameterized with 15- and 20-year internodes in samples 1 and 2, respectively.

Regional growth chronologies are plotted in **Figure 3**. Consistent with the mean height differences between stand generations (**Figure 2**), increases in dominant height growth rate were identified and appeared to be irregular over time. Whereas no clear pattern was evident in the first half century, a noticeable increase occurred in following decades. Growth chronologies also revealed synchronous growth declines in the 2 samples, centred in the 1940s and 1990s, although the first was undetected by the sample 2 spline estimate, but appeared in the growth increments. The decline in the 1990s was also shown to be more acute in sample 2, in which the average growth rate was similar to the

	Model structure		Parameter estimates							
	f_1	f_2, spline internode	$S_{b,0}$ (m/yr)	K_0 (m)	m	$\sigma_{Sb,1}$[a] (m/yr)	$\sigma_{Sb,2}$[a] (m/yr)	$\sigma_{K,1}$[a] (m)	σ (RSE[b]) (m/yr)	λ
Sample 1	Hossfeld	15 years	0.381 (0.023)	49.0 (1.8)	0.667 (0.021)	0.055 (0.024)	0.028 (0.034)	4.9 (0.2)	0.28 (0.09)	0.45 (0.11)
Sample 2[c]	Hossfeld	20 years	0.446	44.3	0.567	0.065	0.030	3.0	0.29	0.63
	Korf	20 years	0.454 (0.024)	45.7 (1.3)	0.588 (0.047)	0.066 (0.023)	0.032 (0.031)	3.1 (0.2)	0.28 (0.08)	0.59 (0.10)

Parameters estimates (continued, f_2)	$d_1 \times 10^2$ (1/year)	$d_2 \times 10^4$ (1/year^2)	$d_3 \times 10^4$ (1/year^3)	$p_1 \times 10^4$ (1/year^3)	p_2	p_3	p_4	p_5	p_6	pm_0	pm_1	pm_2
Sample 1	-0.765 (0.315)	-3.509 (5.946)	0.420 (0.246)	-1.216 (0.468)	1.662 (0.464)	-1.312 (0.482)	0.312 (0.570)	-0.003 (0.954)	9.167 (9.153)	-0.448 (0.484)	0.049 (0.448)	-0.203 (0.272)
Sample 2 (Hossfeld)	0.162	-2.025	0.040	-0.047	0.135	-0.601	1.73	-	-	-0.056	-0.117	0.249
(Korf)	0.196 (0.187)	-1.494 (2.640)	0.028 (0.085)	-0.019 (0.167)	0.120 (0.177)	-0.589 (0.225)	1.728 (0.521)	-	-	-0.027 (0.166)	-0.134 (0.166)	0.253 (0.130)

Table 2. Characteristics and parameter estimates for models of dominant height growth. [a]indexes denote the level of random variation in standard deviation estimates, [b]in the absence of a variance function, [c]The best fit was obtained with the Korf equation for sample 2. The Hossfeld equation fit is also provided for comparison with sample 1, as it was used for elaboration of growth-environment relationships (Tables 3 and 4). Standard-errors of parameter estimates are in parentheses.

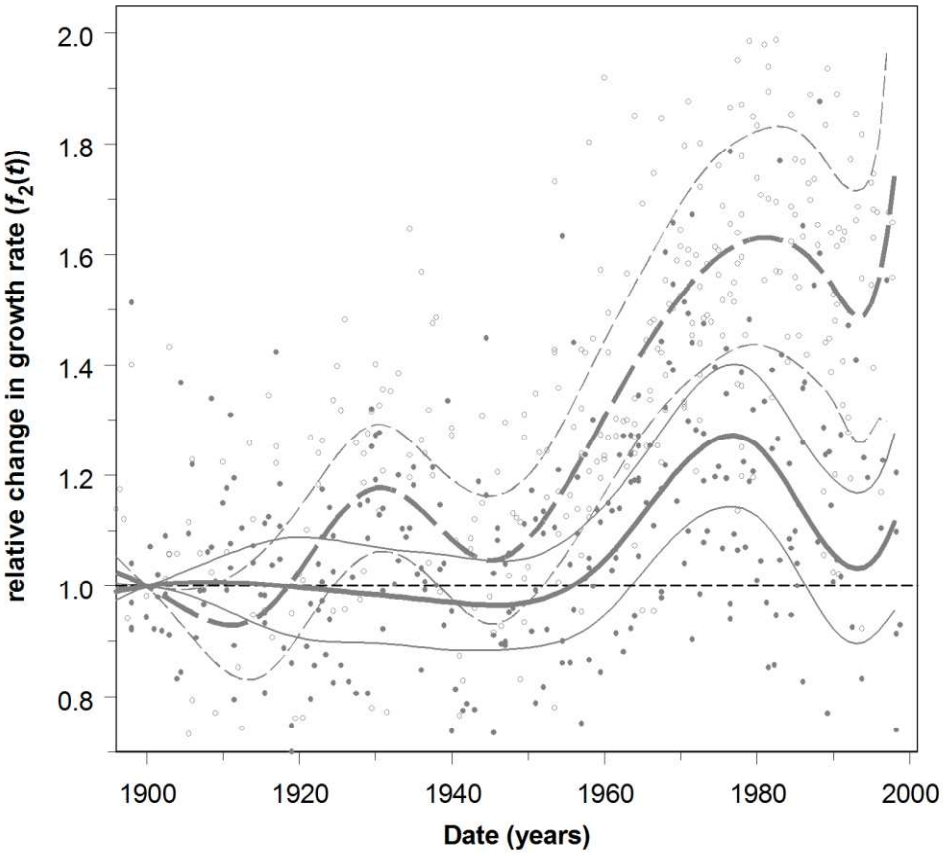

Fig. 3 Regional chronologies of dominant height growth rate. Thick lines: growth chronologies (cubic spline estimates), thin lines: 95% bilateral confidence intervals, circle symbols: growth increments plotted against their median dates. Dashed lines and empty circle symbols: sample 1 (Bontemps et al. 2009), full lines and solid circles: sample 2.

level in 1900. The biggest difference between chronologies was apparent in the intensity of regional changes in growth rate. While the increase in growth rate reached +60% in sample 1 around 1980, it barely reached +30% in sample 2 before flattening off. Hence, the magnitude of change in sample 1 was double that in sample 2. The 95% confidence intervals for the estimated trends stopped overlapping between samples from the 1960s onwards.

Growth-environment relationships

Although the Korf equation provided the best fit for sample 2, the fit for the Hossfeld equation was very close (only +4.5 point difference in AIC). Plot estimates for maximal growth rate (S_b) were thus extracted from a Hossfeld-based model, as in sample 1 (the difference between these estimates was tiny; see Online Resource). Significant correlations between maximal growth rate and environmental indicators are reported in **Table 3**.

Sample 1

We identified negative correlations with soil acidity level (pH, aluminium, Ellenberg indicator for basicity) and positive correlations with soil nutrition indicators, including nitrogen (C:N ratio, Ellenberg indicator for nitrogen), phosphorus and base cation richness (S:CEC ratio and calcium concentration). A single correlation with a water indicator was demonstrated (precipitation in September), suggesting the absence of particular water constraints in the area. There were positive correlations with minimum temperatures in the early growing season (February to June), and strong negative correlations with maximum temperatures in the cold season (October to February). Finally, there was a negative correlation with ambient light (Lel) and summer radiation (June to August). Due to the seasonal patterns detected for temperature and radiation, we computed the following mean indicators (correlations coefficients are given in parentheses): Tn4-5 (+0.40), Tn4-6 (+0.38) and Tn2-6 (+0.40), Tx12-1 (-0.63), Tx12-2 (-0.64), Tx10-1 and Tx10-2 (-0.61), and Rad6-8 (-0.49). We incorporated these indicators into a multiple linear regression model of maximal growth rate following the procedure outlined in the Modelling Approach section. The final regression model is presented in **Table 4**.

Sample 2

We also identified positive correlations with soil nutrition indicators for sample 2, including nitrogen (C:N ratio, Ellenberg indicator for nitrogen) and cation richness (CEC, S:CEC ratio, concentration of base cations and calcium). A negative correlation was found with proton

	Sample 1 (n = 28)	Sample 2 (n = 30)	Samples 1+2 (n = 58)
Nutritional resources			
Acidity level	**pH**$^{(2)}$ (+), **Al** (–), **Rel** (0.46)	**H** (–0.42)	
Nitrogen	**C:N** (–0.38), **C:N**$^{(2)}$ (–0.44), **Nel (0.56)**	**C:N (–0.64)**, **Nel** (0.44)	**C:N (–0.34)**, **Nel** (+)
Phosphorus	**Phos** (0.41)		**Phos (+0.32)**
Cation	**S/T** (0.41), **Ca, Ca**$^{(2)}$ (+)	**CEC** (+), **S** (+), **S/T** (+), **Ca** (+)	**S/T** (+)
Water resources			
Climate	**P9** (–0.37), **WB7** (+)	**P4** (0.38), **P5 (0.47)**, **P6 (0.54), P7 (0.47)** **WB5** (0.38), **WB6** (0.35)	
Soil water budget		**SWC100** (0.34), **Fel** (+) **SWD6 (–0.58)**, **SWD7** (–0.35)	
Energy resources			
Temperature	**Tn2** (0.41), **Tn3** (0.37), **Tn4** (0.42) **Tn5** (0.37), **Tn6** (+)		**Tn all months** (0.34 to 0.55) **Tn (0.54)**
	Tx10 (–0.60), **Tx11** (–0.45), **Tx12 (–0.56)** **Tx1 (–0.66)**, **Tx2 (–0.57)**	**Tx10 (–0.57)**, **Tx11 (–0.59)**, **Tx12 (–0.59) Tx1 (–0.51)**, **Tx** (–0.36)	**Tx9 (–0.36)**, **Tx10 (–0.37)**
Light	**Rad6 (–0.49)**, **Rad7 (–0.53)**, **Rad8** (–0.46) **Lel (–0.65)**	**Rad5** to **Rad7** (0.40)	

Table 3. Correlations between maximal growth rate in dominant height and environmental indicators. Pearson correlation coefficients are in parentheses. $p < 0.01$: numerical correlations in bold, $p < 0.05$: numerical correlations, $p < 0.1$: +/–. Significant correlations were most often established with soil indicators in the first soil layer, otherwise $^{(2)}$ refers to soil layer 2. See Table 1 and text for explanation of abbreviations in Table 3 cells.

concentration. No correlation was found with phosphorus concentration. Positive correlations with indicators of water availability suggested the existence of a water constraint in the region (i.e. precipitation from April to July, water balance in May and June, soil water capacity and Ellenberg indicator for humidity, and soil water deficits in June and July). As in sample 1, we identified a negative effect of maximal temperatures in the cold season (October to January). Lastly, there was a positive effect of spring solar radiation (May to July). We then computed the following temperature averages: Tx11-12 (-0.60), Tx10-12 (-0.50) and Tx10-1 (-0.50). The regression model is presented in **Table 4**.

Samples 1+2

When samples 1 and 2 were combined, positive correlations were confirmed for nitrogen (C:N ratio, Ellenberg indicator for nitrogen), phosphorus concentration, and S:CEC ratio (**Table 3**). Correlations with minimum temperatures were significant for all months, and we retained the mean annual minimum temperature. Negative correlations were found with maximum temperatures in September and October. The final regression model is reported in **Table 4**.

DISCUSSION

Regional chronologies and intensity of productivity changes

A major finding of this study was the strong regional difference in the magnitude of historical evolutions of dominant height growth rate, while temporal patterns were highly similar. The regional variation detected was thus a matter of signal intensity (**Figure 3**). Most of the changes occurred in the second half of the twentieth century and differed by a factor of 2 at their maximum level in the 1980s (+60% and +30% for samples 1 and 2, respectively). The growth decline in the 1990s was stronger in sample 2. The growth increase over time has been progressive reaching +27% and +6% on average in samples 1 and 2 over the twentieth century, respectively. The relationship between dominant height and total stand production (Assmann 1970) suggests similar increases in productivity.

Interestingly, these magnitudes of increase are similar to those of retrospective process-based simulations. For sites spanning a latitudinal gradient in Europe, van Oijen et al. (2008) reported NPP increases ranging from +5 to +20% over the period 1920–2000 as a combined effect of changes in atmospheric CO_2, nitrogen deposition and climate. A simulation of climate change and

Parameter	Estimation		Proportion of variation explained [a]
	estimate	*p*-value	
Sample 1			
Intercept (m yr^{-1})	0.543	0.015	
Tx10-1 (°C) [b]	-0.044	0.020	25.9%
Phos – layer 1 (g kg^{-1})	0.596	0.001	18.6%
N Ellenberg	0.015	0.040	17.1%
Tn4-6 (°C) [b]	0.052	0.023	2.3%
n = 28 , R^2 = 63.9% , RSE = 0.029 (m. yr^{-1})			
Sample 2			
Intercept (m yr^{-1})	0.987	$<10^{-4}$	
C:N – layer 1	-0.011	0.007	19.7 %
Tx11-12 (°C) [b]	-0.050	0.036	11.1 %
SWC100 (mm)	0.0005	0.044	10.2 %
n = 30, R^2 = 41.0% , RSE = 0.047 (m. yr^{-1})			
Samples 1+2			
Intercept (m yr^{-1})	0.846	$<10^{-4}$	
Tn (°C) [b]	0.059	$<10^{-4}$	34.6 %
C:N – layer 1	-0.009	7×10^{-4}	12.2 %
Tx9-10 (°C) [b]	-0.035	0.006	7.8 %
n = 58, R^2 = 54.6%, RSE = 0.050 (m. yr^{-1})			

Table 4. Regressions of maximal growth rate in dominant height against environmental indicators. [a] based on non-sequential (type III) sum of squares, [b] mean temperatures

CO_2 impacts on common beech in northern France for the period 1960–2000 (Loustau et al. 2005) estimated an NPP increase of 13%, a value that is between our 2 estimates.

Environmental interpretation of changes in productivity

The following necessary conditions should be met when attempting to attribute changes in productivity to environmental factors: (i) each putative factor must have experienced variation over time; (ii) temporal patterns of factor(s) and growth should match, assuming that the growth response is not delayed and that growth saturation is not attained (temporal argument); (iii) regional variations in growth changes must follow those of factor(s) (spatial argument), and (iv) the same factor(s) must be identified as limiting for growth, which further requires that no other factor is sufficiently constraining to totally suppress the productivity response (limiting factor argument). The role of each putative environmental factor is now discussed with respect to these conditions. The resulting deductions are summarized in **Table 6**.

Atmospheric carbon dioxide

Atmospheric CO_2 concentration increased from about 295 ppm in 1900 to 370 ppm in 2000, with acceleration in the 1950s, reaching a mean annual progression of 1.2 ppm yr^{-1} during the period 1950–2000 compared to 0.3 ppm yr^{-1} during the period 1900–1950 (CDIAC data). Hence, CO_2 chronology is not contradictory to trends reported. Because there is no spatial variation in CO_2 concentration at these geographic scales (Chahine et al. 2005), its limiting effect on productivity was not testable. To account for regional differences emphasized in growth chronologies, a combined role of either permanent constraints or synergies with other drivers is required (**Table 6**).

Temperature and precipitation

The mean temperature chronology for France (Moisselin et al. 2002) matches northern hemisphere chronology (Jones and Moberg 2003). There was a centennial increase of +1°C, with stability in the period in the 1940-1980s, after which temperature has been steadily rising. The stationary mid-period has been referred to repeatedly since Jones et al. (1982). No significant trend in precipitation has been reported over the last century (Moisselin et al. 2002). Annual anomalies for mean temperature and precipitation (**Figure 4**) are comparable between our samples. Annual fluctuations were higher in sample 1, especially for precipitation.

The main objection to the role of temperatures in measured growth accelerations is the fact that temperatures remained stationary during the period 1950-1980 (**Figure 4**). Growth-environment

4a

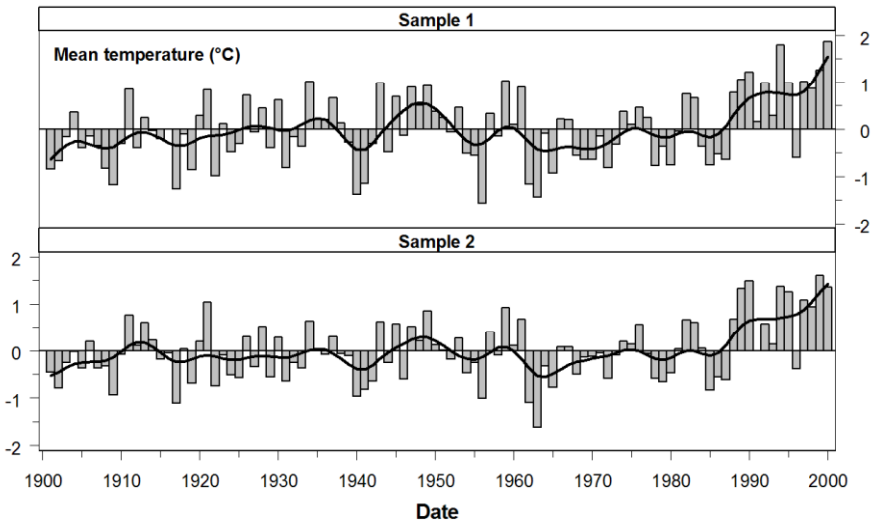

4b

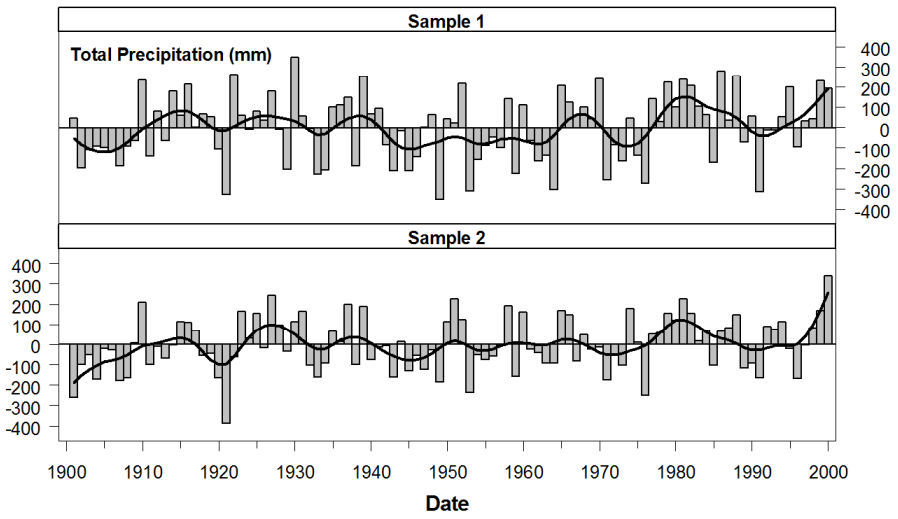

Fig. 4 Anomalies of mean annual temperature and annual precipitation (1901–2000). a: mean annual temperature, b: annual precipitation. Data extracted from Tyndall dataset CRU TS 1.2 for both samples (see Materials). Anomalies were smoothed using spline interpolation (thick line).

relationships further suggest antagonistic effects of temperature (**Table 4**): positive effects of minimum annual temperatures (Tn) and of minimum spring temperatures (Tn4-6) were identified throughout the whole study area and in sample 1 (colder climate than in sample 2). Conversely, a negative effect of maximum cold season temperatures was detected in both samples. Both effects are of comparable magnitude and might have counteracted each other. When combined, these observations invalidate the role of temperature in the growth increases reported (**Table 6**).

Precipitation anomalies (**Figure 4**) followed no long-term trend paralleling productivity increases. In sample 1, no water constraint was identified. In sample 2, where precipitation was lower (**Table 1**), SWC100 was significant in the model of maximal growth rate (**Table 4**). Thus, precipitation was not identified as a low-frequency driver of productivity changes, but may have acted as a permanent constraint in that area.

Nevertheless, singular climatic years may have played a significant role in decennial fluctuations in growth (**Figures 3** and **4**). The positive precipitation anomalies observed for in the 1980s were synchronous with maximum levels of the growth rate. Growth declines were also synchronous with exceptional successions of warm years during the periods 1943-1949 and 1989-2000. Exceptional tree mortality following droughts in the period 1947-49 has also been reported for common beech in France (Schaeffer 1955). Lower water availability in sample 2 (**Tables 1** and **3**) may also have resulted in a greater impact of dry years during the 1990s and may explain the higher intensity of the observed decline (**Table 6**).

Nitrogen availability and nitrogen deposition

A comprehensive record of past nitrogen deposition is lacking. However, there is a consensus that the mid-twentieth century increase tracked the course of emissions resulting from increasing fossil fuel combustion and fertilizer use in Europe (Asman and Drukker 1988; Holland et al. 2005). This is corroborated by existing measurements (Blake et al. 1999), ice-core records (Hastings et al. 2009) and vegetation reconstitutions (Pitcairn et al. 1995). In France, the Alpine ice-core reconstitution of atmospheric nitrate (Preunkert et al. 2003) also agrees with the records. Our reported evolutions in growth rate would thus be temporally consistent with the course of nitrogen deposition (temporal argument, **Table 6**).

Despite regional differences in nitrogen status (**Table 1**), we determined a significant positive effect of current nitrogen availability on growth (using both vegetation-related and soil indicators) in each sample and in the combined dataset (**Table 4**). Hence, nitrogen is identified as a limiting factor, even in the better nutritional conditions of sample 1, which is consistent with the findings of Seynave et al. (2008) for common beech (limiting factor argument, **Table 6**).

	Sample 1	Sample 2	Difference (%) (sample 1)
Elevation (m a.s.l.)	371 (48)	125 (51)	
Annual precipitation 1993-1998 (mm)	825 (60)	670 (52)	
NO_3^--N (kg ha^{-1} yr^{-1})	3.3 (0.1)	2.6 (0.2)	+28%
NH_4^+-N (kg ha^{-1} yr^{-1})	5.4 (0.2)	3.8 (0.4)	+44%
Total N (kg ha^{-1} yr^{-1})	8.9 (0.3)	6.5 (0.6)	+37%

Table 5. Modelled average level of bulk nitrate, ammonium and total nitrogen deposition for the period 1993–1998 for growth samples. Deposition levels were computed from models of NH_4-N, NO_3-N and total N bulk deposition calibrated from the RENECOFOR monitoring network (ICP forests) as a function of elevation, monthly precipitation and period of the year (Croisé et al. 2005). Standard deviations are given in parentheses.

Bulk nitrogen deposition levels predicted over the two samples remain moderate, as they do not exceed 10 $kg.ha^{-1}.yr^{-1}$ (**Table 5**; Ulrich 1999). However, bulk deposition in the open field generally underestimates total deposition to the ecosystem (Dämmgen et al. 2005; Ulrich 1999), in general by 20-30% (Croisé et al. 2005). Average 1993-1998 bulk deposition levels of nitrate and ammonium were found higher in sample 1 (**Table 5**), which had a very significant +37% total nitrogen deposition excess over sample 2 ($p = 7\ 10^{-11}$). This regional pattern has been found consistent with levels of precipitation higher in north-eastern than in north-western France (**Table 1**; Croisé et al. 2005), as observed on the CATANEAT monitoring network (Ulrich 1999). Given the known determinants of nitrogen deposition (emission hotspots, topography, climatic conditions), this predicted difference may have been in effect over a longer time scale. Thus, it is in accordance with the regional differentiation of productivity changes (spatial argument, **Table 6**), and it may have increased the regional difference in soil richness and nitrogen status (see Materials and **Table 1**). As the study was carried out on temporary plots, we used modelled data of bulk nitrogen deposition. Despite these models have shown a good predictive ability (Croisé et al. 2005), these predictions remain subject to uncertainty. In addition, total bulk deposition in the open field does not take canopy interception and exchanges into account (Draajers et al. 1997). For these reasons, predicted nitrogen deposition levels and their regional difference may only deliver a rough picture of real deposition to the forest stands sampled.

Environmental change	Temporal argument Consistency of historical variations with growth chronologies on the long-term	Spatial argument Consistency with regional differentiation of growth chronologies	Limiting factor argument Constraint from growth-environment relationships	Conclusion
Atmospheric CO_2	**YES** (CDIAC datasets)	No regional variation (Chahine et al. 2005)	Impossible to determine by observation	**Compatible** Cannot have acted alone
Temperature	NO (Figure 4) Warm events may account for 1940s and 1990s growth declines	NO (Figure 4)	Antagonistic effects evidenced (Tables 3 and 4)	**Rejected** **Role in short-term events**
Precipitation	No long-term variation (Figure 4) Wet events may account for growth increase in the 1980s	NO (Figure 4)	**YES** in sample 2 (Table 3 and 4)	**Rejected** **Role in short-term events** May be a permanent constraint in sample 2
Nitrogen	**YES** (French Alps chronology, Preunkert et al. 2003)	**YES** (Table 5)	**YES** in both samples (Tables 3 and 4) may be more pronounced in sample 2	**Compatible**

Table 6. Compatibility of environmental changes with long-term growth changes in common beech. Tables, figures or growth sources supporting the analysis are in parentheses.

Because no significant negative effect of acidity indicators was detected (though some trends were apparent sample 1), the eutrophicating role of nitrogen deposition may have overruled its acidifying side effect (Macdonald et al. 2002). Less acidic soil conditions in sample 1 (**Table 1**) may have also prevented such an impact. In addition, deposition levels were below the threshold of 10 kg ha^{-1} yr^{-1}, above which nitrogen leaching and saturation may be triggered (Dise and Right 1995). Our results thus support the existence of nitrogen limitation during the past century (Johnson 2006) and a growth enhancement by nitrogen deposition (**Table 6**).

Additional roles of regional environmental constraints and local events

Nutritional and water resources were less favourable in sample 2 (**Table 1**), and both were shown to influence growth (**Table 4**). The SWC100 was the single significant water indicator in the regression model of maximal growth rate, but spring/summer precipitation and water balances were positively correlated with maximal growth rate (water deficits in summer negatively correlated), which was not the case in sample 1 (**Table 3**). Therefore, as a permanent constraint, lower water availability may have hindered the productivity response in the area. However, other constraints were found to be specific to sample 1, such as phosphorus limitation (Phos) and minimum temperatures in the early growing season (Tn4-6). While soil concentrations were equivalent in samples 1 and 2, phosphorus limitation in sample 1 may be interpreted as the indication of a shift in growth control following increased nitrogen availability. This finding is consistent with the progressive phosphorus limitation evidenced in recent nitrogen fertilization experiments (Braun et al. 2009).

In the Atlantic beech forest domain, unusual tree mortality has been reported in the period 1965-1980, as ensuing from a simultaneous attack of the insect *Cryptococcus fagisuga* and the fungus *Nectria coccinea*. Mortality was exacerbated in the years following the drought event in 1976 (Mormiche 1994). While forest declines occurred in 3 of the forests we sampled (Lyons, Eawy and Eu, see Table 1 in Online Resource), increased height growth over this period (**Figure 3** and pair-wise height comparisons in these forests) suggests, either that these stands were not impacted at all by these disturbances, or that any resulting tree mortality may not have lowered between-tree competition to the point that height growth of the surviving trees would have been reduced.

CONCLUSIONS

We report increases in common beech productivity after the mid-twentieth century and their parallel course with strong differentiation in 2 regions of contrasting nutritional status. Growth and temperature chronologies did not match over the long term. Growth chronologies were consistent with CO_2 chronology, but CO_2 alone cannot account for the regional difference emphasized. The clearest environmental signal was related to nitrogen. This factor met the requirements of temporal and spatial concordance with growth chronologies, and was also identified as limiting for growth. Nitrogen/CO_2 interaction was not contradicted by our observations, but could not be tested. Short-term anomalies in precipitation and temperature, including recent climate warming, may have played roles in productivity declines in the 1940s and 1990s and in the productivity peak in the 1980s. Water constraint evidenced in north-western France may have also contributed to this regional differentiation.

Our results thus extend observations on the role of nitrogen over the medium- (Kahle et al. 2008a; Nellemann and Thomsen 2001) and short-terms (Solberg et al. 2009) and the inferences of FACE experiments including nitrogen addition (Nowak et al. 2004). They are also compatible with retrospective process-based modelling explorations of the role of nitrogen in the productivity of evergreen species in Europe (van Oijen et al. 2008). It is remarkable that past increases in NPP simulated for common beech in France (Loustau et al. 2005) showed no regional differentiation when nitrogen deposition was not taken into account, and were of a smaller magnitude than reported for the north-eastern area.

A comparison of retrospective process-based simulations and observations of past productivity changes remain crucial to further improve our understanding of the environmental origins of these changes. This comparison would also allow testing of the predictive accuracy of process-based models over the long-term (Pussinen et al 2009). However, retrospective modelling explorations of environmental change impacts on productivity are still insufficient (Hasenauer et al. 1999, van Oijen et al. 2008). Furthermore, combinations of simulation and observation remain rare (Kahle et al 2008a). Because the parameterisation of process-based models most often requires intensive measurements of simulated forest plots, rapid progress seems unlikely. One option may lie in the use of more parameter-sparse hybrid modelling approaches that combine process-based and statistical models of forest dynamics (Landsberg 2003; Matala et al. 2006).

ACKNOWLEDGEMENTS

The authors gratefully thank the French Ministry for Agriculture and Fisheries (MAP) and the French Forest Service (ONF) for providing funding and support to the present study. They also wish to thank Antoine Cazin (INRA), Jérôme Piat (ONF) and several ONF services for their helpful assistance in the sampling phase, Daniel Rittié (INRA) for conducting stem analyses, Vincent Perez (AgroParisTech) for climate data extraction, Erwin Ulrich and Manuel Nicolas (ONF) for useful discussions on nitrogen deposition measurements and associated models, and Jean-Claude Pierrat (INRA) and the two anonymous reviewers that greatly helped in clarifying the manuscript.

Reference list

Aber JD, McDowell W, Nadelhoffer KJ et al (1998) Nitrogen saturation in temperate forest ecosystems - Hypotheses revisited. Bioscience 48:921-934

Aber JD, Goodale CL, Ollinger SV et al (2003) Is nitrogen deposition altering the nitrogen status of northeastern forests? BioScience 53:375-389

Andrianarisoa KS, Zeller B, Dupouey J-L, Dambrine E (2009) Comparing indicators of N status of 50 beech stands (*Fagus sylvatica* L.) in northeastern France. For Ecol Manage 257:2241-2253

Asman W, Drukker B (1988) Modelled historical concentrations and depositions of ammonia and ammonium in Europe. Atmospheric Environ 22:725-735

Assmann E (1970) The principles of forest yield study. Pergamon Press, Oxford

Bénichou P, Le Breton P (1987) Prise en compte de la topographie pour la cartographie des champs pluviométriques statistiques. La Météorologie 7:23-34

Blake L, Goulding WT, Mott CJB, Johnston AE (1999) Changes in soil chemistry accompanying acidification over more than 100 years under woodland and grass at Rothamstead Experimental Station, UK. Eur J Soil Sci 50:401-412

Boisvenue C, Running SW (2006) Impacts of climate change on natural forest productivity - evidence since the middle of the 20th century. Global Change Biol 12:862-882

Bontemps J-D, Hervé J-C, Dhôte J-F (2009) Long-term changes in forest productivity: a consistent assessment in even-aged stands. For Sci 55:549-564

Bormann BT, Gordon JC (1984) Stand density effects in young Red Alder plantations: productivity, photosynthate partitioning and nitrogen fixation. Ecology 65:394-402

Bouriaud O, Breda N, Dupouey JL, Granier A (2005) Is ring width a reliable proxy for stem-biomass increment? A case study in European beech. Can J For Res 35:2920-2933

Braun S, Thomas VFD, Quiring R, Flückiger W (2009) Does nitrogen deposition increase forest production? The role of phosphorus. Env Poll 158:2043-2052.

Chahine M, Barnet C, Olsen ET, Chen L, Maddy E (2005) On the determination of atmospheric minor gases by the method of vanishing partial derivatives with application to CO_2. Geophys Res Lett 32:L23801 doi:10.1029/2005GL024165

Constable JVH, Friend AL (2000) Suitability of process-based tree growth models for addressing tree response to climate change. Env Poll 110:47-59.

Croisé L, Ulrich E, Duplat P, Jacquet O (2005) Two independent methods for mapping bulk deposition in France. Atmospheric Environ 39:3923-3941.

Curtis RO (1964) A stem analysis approach to site index curves. For Sci 10:241-256

Dämmgen U, Erisman JW, Cape JN, Grünhage L, Fowler D (2005) Practical considerations for addressing uncertainties in monitoring bulk deposition. Env Poll 134:535-548

Dise NB, Wright RF (1995) Nitrogen leaching from European forests in relation to nitrogen deposition. For Ecol Manage 71:153-161

Draaijers GPJ, Erisman JW, van Leeuwen NFM, Römer FG, Te Winkel BH, Veltkamp AC, Vermeulen AT, Wyers GP (1997) The impact of canopy exchange on differences observed between atmospheric deposition and throughfall fluxes. Atmospheric Environ 31:387-397

Duplat P, Tran-Ha M (1997) Modelling of dominant height growth in Sessile oak (Quercus petraea Liebl) in France. Regional variability and effect of the recent period (1959-1993). Ann For Sci 54:611-634

Ellenberg H, Weber HE, Düll R, Wirth V, Werner W, Paulissen D (1992) Zeigerwerten von pflanzen in Mitteleuropa. Scripta Geobotanica 18:1-248

Esper J, Cook ER, Schweingruber FH (2002) Low-frequency signals in long tree-ring chronologies for reconstructing past temperature variability. Science 295:2250-2252

European Commission. (2005) Soil Atlas of Europe. European Soil Bureau Network, Luxembourg

Hasenauer H, Nemani RR, Schadauer K, Running SW (1999) Forest growth response to changing climate between 1961 and 1990 in Austria. For Ecol Manage 122: 209-219

Hastings MG, Jarvis JC, Steig EJ (2009) Anthropogenic impacts on nitrogen isotopes of ice-core nitrate. Science 324:1288

Hendrey GR, Ellsworth DS, Lewin KF, Nagy J (1999) A free-air enrichment system for exposing tall forest vegetation to elevated atmospheric CO_2. Global Change Biol 5:293-309

Högberg P, Fan HB, Quist M, Binkley D, Tamm CO (2006) Tree growth and soil acidification in response to 30 years of experimental nitrogen loading on boreal forest. Global Change Biol 12:489-499

Holland EA, Braswell BH, Sulzman J, Lamarque J-F (2005) Nitrogen deposition onto the United States and Western Europe: synthesis of observations and models. Ecol Appl 15:38-57

Hyvönen R, Ågren GI, Linder S et al (2007) The likely impact of elevated [CO_2], nitrogen deposition, increased temperature and management on carbon sequestration in temperate and boreal forest ecosystems: a literature review. New Phytol 173:463-480

Jacoby GC, D'Arrigo RD (1997) Tree rings, carbon dioxide, and climatic change. PNAS USA 94:8350-8353

Janssen BH (1996) Nitrogen mineralization in relation to C:N ratio and decomposability of organic materials. Plant Soil 181:39-45

Johnson DW (2006) Progressive N limitation in forests: review and implications for long-term responses to elevated CO_2. Ecology 87:64-75

Jones PD, Wigley TML, Kelly PM (1982) Variations in surface air temperatures : Part 1. Northern hemisphere, 1881-1980. Month Weather Rev 110:59-70

Jones PD, Moberg A (2003) Hemispheric and Large-Scale Surface Air Temperature Variations: An Extensive Revision and an Update to 2001. J Climate 16:206-223

Kahle HP, Karjalainen T, Schuck A, Agren GI (eds) (2008a) Causes and consequences of forest growth trends in Europe. EFI, Joensuu

Kahle HP, Spiecker H, Unseld R et al (2008b) Temporal trends and spatial patterns of height growth changes in relation to changes in air temperature and precipitation, and in relation to levels of foliar nitrogen and nitrogen deposition. In: Kahle H-P, Karjalainen T, Schuck A et al (eds) Causes and consequences of forest growth trends in Europe, Research Report 21, EFI, Joensuu, pp 127-167

Körner C, Asshoff R, Bignucolo O et al (2005) Carbon flux and growth in mature deciduous forest trees exposed to elevated CO_2. Nature 309:1360-1362

Lamarche VC, Graybill DA, Fritts HC, Rose MR (1984) Increasing atmospheric carbon dioxide: tree ring evidence for growth enhancement in natural vegetation. Science 225:1019-1021

Landsberg J (2003) Physiology in forest models: history and the future. FBMIS 1:49-63.

Lanner RM (1985) On the insensitivity of height growth to spacing. For Ecol Manage 13:143-148

Lindström MJ, Bates DM (1990) Nonlinear mixed effect models for repeated measures data. Biometrics 46:673-687

Loustau D, Bosc A, Colin A et al (2005) Modeling climate change effects on the potential production of French plains forests at the sub-regional level. Tree Physiol 25:813-823

Luckai N, Laroque GR (2002) Challenges in the application of existing process-based models to predict the effect of climate change on C pools in forest ecosystems. Climatic Change 55:39-60

Macdonald JA, Dise NB, Matzner E, Armbruster M, Gundersen P (2002) Nitrogen input together with ecosystem nitrogen enrichment predict nitrate leaching from European forests. Global Change Biol 8:1028-1033

Mäkelä A, Landsberg J, Ek AR, Burk TE, Ter-Mikaelian M, Ågren G, Oliver CD, Puttonen P (2000) Process-based models for forest ecosystem management : current state of the art and challenges for practical implementation. Tree Physiol 20:289-298

Matala J, Ojansuu R, Peltola H, Raitio H, Kellomäki S (2006) Modelling the response of tree growth to temperature and CO2 elevation as related to the fertility and current temperature sum of a site. Ecol Model 199:39–52

Medlyn B, McMurtrie RE, Dewar R, Jeffreys MP (2000) Soil processes dominate the long-term response of forest net primary productivity to increased temperature and atmospheric CO_2 concentration. Can J For Res 30:873-888

Mitchell TD, Carter TR, Jones PD, Hulme M, New M (2004) A comprehensive set of high-resolution grids of monthly climate for Europe and the globe : the observed records (1901-2000) and 16 scenarios (2001-2100). Research Working paper 55, Tyndall Centre for Climate Change, Norwich, 25p

Moisselin JM, Schneider M, Canellas C, Mestre O (2002) Climatic changes in France during the 20th century. Analysis of long homogenised time series of temperature and precipitation [In French]. La Météorologie 38:45-56

Mormiche A (1994) Managing forest decline of common beech in Normandy 1961-1988 (in French). Revue Forestière Française 46: 586-590

Nadelhoffer KJ, Emmett BA, Gundersen P et al (1999) Nitrogen deposition makes a minor contribution to carbon sequestration in temperate forests. Science 398:145-148

Nellemann C, Thomsen MG (2001) Long-term changes in forest growth: potential effects of nitrogen deposition and acidification. Water, Air Soil Poll 128:197-205

Norby RJ, DeLucia EH, Gielen B et al (2005) Forest response to elevated CO_2 is conserved across a broad range of productivity. PNAS USA 102:18052-18056

Nowak RS, Ellsworth DS, Smith SD (2004) Functional responses of plants to elevated atmospheric CO2 - do photosynthetic and productivity data from FACE experiments support early predictions? New Phytol (Tansley Review) 162:253-280

van Oijen M, Agren GI, Chertov O et al (2008) Evaluation of past and future changes in European forest growth by means of four process-based models. In: Kahle HP, Karjalainen T, Schuck A et al (eds) Causes and consequences of forest growth trends in Europe, Research Report 21, EFI, Joensuu, pp 183-199

Ollinger SV, Aber JD, Reich PB, Freuder R (2002) Interactive effects of nitrogen deposition, tropospheric ozone, elevated CO_2 and land use history on the carbon dynamics of northern hardwood forests. Global Change Biol 8:545-562

Piedallu C, Gégout J-C (2007) Multiscale computation of solar radiation for predictive vegetation modelling. Ann For Sci 64:899-909

Pinheiro JC, Bates DM (2000) Mixed-effects models in S and S-PLUS. Springer, New-York

Pitcairn CER, Fowler D (1995) Deposition of fixed atmospheric nitrogen and foliar nitrogen content of Bryophytes and Calluna vulgaris (L.) Hull. Env Poll 88:193-205

Polge H (1981) The influence of thinnings on the growth constraints of Beech (in French). Ann For Sci 38: 407-423

Preunkert S, Wagenbach D, Legrand M (2003) A seasonally resolved alpine ice core record of nitrate : Comparison with anthropogenic inventories and estimation of preindustrial emissions of NO in Europe. J Geophys Res 108: doi:4610.1029/2003JD003475

Pussinen A, Nabuurs GJ, Wieggers HJJ, et al (2009) Modelling long-term impacts of environmental

change on mid- and high-latitude European forests and options for adaptive forest management. For Ecol Manage 258: 1806-1813

Schaeffer A (1955) Decline in common beech in the administrative unit of Doubs (in French). Bull d Soc Forest Franche-Comté 28: 290-291

Schaffers AP, Sýkora KV (2000) Reliability of Ellenberg indicator values for moisture, nitrogen and soil reaction: a comparison with field measurements. J Veg Sci 11:225-244

Seynave I, Gégout J-C, Hervé J-C, Dhôte J-F (2008) Is the spatial distribution of European beech (*Fagus sylvatica* L.) limited by its potential height growth? J Biogeog 35:1851-1862

Solberg S, Dobbertin M, Reinds GJ et al (2009) Analyses of the impact of changes in atmospheric deposition and climate on forest growth in European monitoring plots: a stand growth approach. For Ecol Manage 258:1735-1750

Spiecker H, Mielikäinen K, Köhl M, Skovsgaard JP (eds) (1996) Growth trends in European forests. Springer-Verlag, Berlin Heidelberg

Ulrich E (1999) Estimation of nitrogen deposition on 27 RENECOFOR plots (France) from 1993 to 1996. In: Karjalainen T, Spiecker H, Laroussinie O (eds) Causes and consequences of accelerating tree growth in Europe, Proceedings 27, EFI, Joensuu, pp 139-156

Wright RF, Rasmussen L (1998) Introdution to the NITREX and EXMAN projects. For Ecol Manage 101:1-7

Zeide B (1993) Analysis of growth equations. For Sci 39:594-616

Online Resource

Nitrogen footprint in a long-term observation of forest growth over the twentieth century. Trees – structure and function

Jean-Daniel BONTEMPS, AgroParisTech, ENGREF, UMR 1092 INRA/AgroParisTech Laboratoire d'Etude des Ressources Forêt-Bois (LERFoB), 14 rue Girardet, 54000 Nancy, France. jean-daniel.bontemps@engref.agroparistech.fr

Jean-Christophe HERVÉ, Inventaire Forestier National (IFN), Direction Technique, Domaine des Barres, 45290 Nogent-sur-Vernisson, France. jean-christophe.herve@ifn.fr

Jean-Michel LEBAN, INRA, UMR 1092 INRA/AgroParisTech Laboratoire d'Etude des Ressources Forêt-Bois (LERFoB), Centre de Nancy, 54280 Champenoux, France. leban@nancy.inra.fr

Jean-François DHÔTE, Office National des Forêts (ONF), Direction Technique et Commerciale Bois, Boulevard de Constance, 77300 Fontainebleau, France. jean-francois.dhote@onf.fr

Corresponding author: Jean-Daniel BONTEMPS, jean-daniel.bontemps@engref.agroparistech.fr

1. Location and age of stands (sample 2)

Stand pair	Forest	Location [1]	Elevation [2] (m)	Within-pair distance (km)	Age [3] (years)		Age difference
					Youngest	Oldest	
1	Compiègne	2°55' E 49°24' N	55	7.53	65	111	46
2	Compiègne	2°53' E 49°23' N	50	8.18	66	145	79
3	Compiègne	2°57' E 49°21' N	130	2.16	54	144	90
4	Compiègne	2°53' E 49°19' N	140	3.36	70	165	95
5	Halatte	2°39' E 49°17' N	145	0.52	45	126	81
6	Lyons	1°29' E 49°23' N	155	2.55	94	200	106
7	Lyons	1°35' E 49°27' N	180	1.51	91	178	87
8	Brotonne	0°44' E 49°26' N	115	8.85	77	147	70
9	Brotonne	0°40' E 49°25' N	115	2.20	61	134	73
10	Brotonne	0°44' E 49°27' N	50	1.82	136	176	40
11	Verte	1°07' E 49°30' N	165	3.56	84	143	59
12	Eawy	1°18' E 49°42' N	195	4.77	50	137	87
13	Arques	1°12' E 49°53' N	125	0.77	47	127	80
14	Eu	1°33' E 49°55' N	200	4.70	100	171	71
15	Crécy	1°50' E 50°15' N	65	3.21	113	152	39
Mean			125	3.71	76.9	150.4	73.5
Standard deviation			50	2.54	26.2	23.6	20.0

[1] Mean geographic coordinates of stand pairs (ED 50 system), [2] mean elevation of stand pairs (a.s.l.), [3] stand age in 1998

2. Growth equations tested

Differential expressions of growth equations (f_1)

Equations parameterised with K as the height asymptote (metres) and S_b as the maximal growth rate (metres/year):

– Richards:
$$\frac{dH_0}{dt} = S_b\, C_m \left(\frac{H_0}{K}\right)^{1-m} \left[1-\left(\frac{H_0}{K}\right)^{m}\right]$$

where $C_m = (1\text{-}m)^{(m-1)/m} / m$

– Hossfeld:
$$\frac{dH_0}{dt} = S_b\, C_m \left(\frac{H_0}{K}\right)^{1-m} \left[1-\frac{H_0}{K}\right]^{1+m}$$

where $C_m = 4\,(1-m)^{m-1}\,(1+m)^{-(1+m)}$

- Korf:
$$\frac{dH_0}{dt} = S_b\, C_m \frac{H_0}{K} \left[ln\,\frac{K}{H_0}\right]^{1+m}$$

where $C_m = exp\,[\,(1+m)\;(1-\;ln\,(1+m))\,]$

Expressions for the integrated form (F_1^{-1})

All equations admit close-form solutions for F_1 and F_1^{-1} (integration on time interval $[t_{-1}, t]$):

- Richards:
$$H_0(t) = K\left[1+\left[\left(\frac{H_0(t_{-1})}{K}\right)^{m}-1\right]\exp\left[-\frac{R_b\, m\, C_m}{K}\left(F_2(t)-F_2(t_{-1})\right)\right]\right]^{\frac{1}{m}}$$

- Hossfeld:
$$H_0(t) = \frac{K}{1+\left[\frac{R_b\, m\, C_m}{K}\left(F_2(t)-F_2(t_{-1})\right)+\left(\frac{H_0(t_{-1})}{K-H_0(t_{-1})}\right)^{m}\right]^{-\frac{1}{m}}}$$

- Korf:
$$H_0(t) = K\exp\left[-\left(\frac{R_b\, m\, C_m}{K}\left(F_2(t)-F_2(t_{-1})\right)+\left[\ln\frac{K}{H_0(t_{-1})}\right]^{-m}\right)^{-\frac{1}{m}}\right]$$

where $F_2 = \int f_2(v)\, dv$.

3. Cubic spline function of date (f_2)

Cubic spline functions are piecewise continuous polynomials defined on successive time intervals. These time intervals – or internodes – were set equal along calendar date. Different internodes were tested to assess decennial-order fluctuations (20, 15 and 10 years). The general expression is:

$$f_2(u) = 1 + \mathrm{d}_1 u + \mathrm{d}_2 u^2 + d_3 u^3 + \sum_{\mathrm{k}=1}^{k_1} \mathrm{p}_{\mathrm{k}} \left[max\left(u - n\,\mathrm{k}, 0\right)\right]^3 + \sum_{k=0}^{k_2} \mathrm{pm}_{\mathrm{k}} \left[min\left(u + n\,\mathrm{k}, 0\right)\right]^3$$

where $u = t - t_b$, d_1, d_2, d_3, p_k and pm_k are spline parameters to be estimated, $[0, n]$ is the base internode of spline (n = 20, 15 or 10), and n, k_1 and k_2 externally specify the width and number of spline intervals necessary to describe the entire period range covered. For instance with n = 15, nodes are located at dates 1870, 1885, 1900, 1915, …, 1990.

4. Growth-environment relationships – S_b estimates for sample 2

In sample 2, the best fit was obtained with the Korf equation. However, the difference was only -4.5 AIC units compared with the Hossfeld equation, also the most accurate in sample 1. For a clear comparison of regional growth-environment relationships, S_b estimates were extracted from a Hossfeld-based model in sample 2.

Differences in S_b estimates from Korf- and Hossfeld- based models were investigated (see Figure below). The correlation between both estimates was 1^{-} (p = 0). When Hossfeld S_b estimates were predicted from the Korf ones using simple linear regression, the intercept was not significant: $S_{b,Hossfeld}$ = 0.9816; $S_{b,Korf}$ (RSE = 2.5 10^{-3} m/year). Furthermore, the growth-environment relationship in sample 2 was insensitive to the set of S_b estimates considered.

Comparison of level 2 S_b estimates from a Korf- and Hossfeld-based model